J Coast Conserv (2008) 12:93–104
DOI 10.1007/s11852-008-0034-7

Variability and predictability of sea-level extremes in the Hawaiian and U.S.-Trust Islands—a knowledge base for coastal hazards management

Md. Rashed Chowdhury · P.-S. Chu · Thomas A. Schroeder · Xin Zhao

Received: 29 May 2008 / Revised: 30 October 2008 / Accepted: 2 November 2008 / Published online: 15 November 2008

Abstract The objective of this study is to provide an improved climatology of sea level extremes on seasonal and long-term time scales for Hawaii and the U.S-Trust islands. Observations revealed that the Hawaiian and U.S.-Trust islands, by and large, display a strong annual cycle. For estimating the statistics of return period, the three-parameter generalized extreme value (GEV) distribution is fitted using the method of *L*-moments. In the context of extremes (20- to 100-year return periods), the deviations in most of the Hawaiian Islands (except at Nawiliwili and Hilo) displayed a moderate sea-level rise (i.e., close to 200 mm), but the deviations in the U.S.-Trust islands displayed a considerably higher rise (i.e., more than 300 mm) in some seasons due to typhoon-related storm surges. This rise may cause damage to roads, harbors, and unstable sandy beaches. Correlations between the El Niño-Southern Oscillation (ENSO) climate cycle and the variability of seasonal sea level have been investigated. Results show that correlation for the station located west of the International Date Line (DL) is strong, but it is moderate or even weaker for stations east of the DL. The skill of SST-based Canonical Correlation Analyses (CCA) forecasts was found to be weak to moderate (0.4–0.6 for Honolulu, Kahului, Hilo, and Wake, and 0.3 or below for Kahului, Mokuoloe, and Johnston). Finally, these findings are synthesized for evaluating the potential implications of sea level variability in these islands.

Keywords Sea-level extreme · Coastal hazards · El Niño-Southern Oscillation (ENSO) · Sea-surface temperature (SST) · Hawaii and U.S.-Trust islands

Md. R. Chowdhury (✉)
Pacific ENSO Applications Climate Center (PEAC),
Joint Institute for Marine and Atmospheric Research (JIMAR),
University of Hawaii at Manoa,
2525 Correa Road, HIG 350,
Honolulu, Hawaii 96822, USA
e-mail: rashed@hawaii.edu

P.-S. Chu
Department of Meteorology, School of Ocean and Earth Science and Technology (SOEST), University of Hawaii at Manoa,
Honolulu, USA

T. A. Schroeder
Joint Institute for Marine and Atmospheric Research (JIMAR),
School of Ocean and Earth Science and Technology,
University of Hawaii at Manoa,
Honolulu, USA

X. Zhao
Department of Information and Computer Science,
University of Hawaii at Manoa,
Honolulu, Hawaii, USA

Introduction

Besides being at risk from four natural phenomena—earthquake, volcanic eruptions, tsunamis, and hurricanes—Hawaii is also threatened by coastal erosion, sea-level rise, coastal stream flooding, and extreme seasonal high wave energy (Richmond et al. 2001). Examples of some common coastal Hazards in Hawaii are presented in Fig. 1. The occurrence of these dangerously high water levels and associated erosion and inundation is an extremely important issue. Because all coastal activities are influenced by temporal fluctuations in sea level, there is a demand for information related to variability and predictability of sea-level on seasonal-to-long time scales. This study is therefore aimed at providing a basis for the development

Fig. 1 Common coastal hazards in Hawaii. (Source: http://www.soest.hawaii.edu/coasts/presentations/)

of a seasonal-to-long-term outlook on sea-level variability and predictability for the Hawaiian and U.S.-Trust Islands. This information is significant to decision analyses for coastal hazard management.

In order to examine sea-level variability, the monthly mean values of sea level have been used to investigate the seasonality; the varying likelihood of extremely high sea levels has been examined from the hourly sea-level data. The Generalized Extreme Value (GEV) model is used to estimate the returns of expected extremes of high sea level [details of GEV, L-moments, and bootstrap analyses are available in Gnedenko 1943; Efron and Tibshirani 1993; Chu and Wang 1997; Zwiers and Kharin 1998; Katz et al. 2002; Mendez et al. 2007; and Chu et al. 2008]. Some results of GEV analyses used herein are from the previous work of Chowdhury et al. (2008). These results show that the extreme events in these islands vary both temporally and spatially; some of the islands (Wake and Johnston) display considerably higher extreme values in some seasons on a 1–100-year return period (RP). These seasonal increases are likely to cause tidal inundations followed by increased erosion of these low-lying atolls/islands that result in considerable damage to roads, harbors, unstable sandy beaches, and other major infrastructures.

The predictability of sea-level has been investigated from the ENSO climate cycle and the SSTs in the tropical Pacific Ocean. Many previous studies [see Bjerknes 1966, 1969; Ropelewski and Halpert 1987; Chu 1995; Chu and Chen 2005; Barnston and He 1996; Yu et al. 1997; Chowdhury et al. 2007a, b and references therein] have demonstrated that ENSO has a significant impact on climate variability in the Pacific islands. Two factors (i.e., ENSO and SST) are chosen for forecasting sea-level variability on seasonal time scales, and an operational Canonical Correlation Analyses (CCA) model for seasonal sea-level forecasts has been developed. The monthly average sea level shows a moderate-to-marginal negative deviation during strong El Niño years and a positive deviation during strong La Niña years. While other studies (Chowdhury et al. 2007a) have shown that the sea-level variability in the U.S.-Affiliated Pacific Islands (USAPI) is strongly correlated to ENSO climate cycle, the sea-level variability in the Hawaiian and U.S-Trust islands is found to be weakly-to-moderately correlated to ENSO. Finally, the results are compared and evaluated with respect to the global sea-level rise, reports of the Intergovernmental Panel for Climate Change (IPCC) are discussed, and a scenario for potential implications of sea-level extremes is presented.

Data

The research-quality, hourly sea-level data for the years with at least 4-month of data have been used for the extreme-value analyses. All these sea-level heights have been referred to the tide staff's zero, which is linked to fixed benchmarks.

In order to investigate the seasonality of the sea-level variability, the seasonal average data for the following Hawaiian stations (Honolulu, Kahului, Mokuoloe, Nawiliwili, and Hilo) and U.S-Trust stations (Wake and Johnston) (Fig. 2) have been analyzed (Source: University of Hawaii Sea Level Center (UHSLC), available at http://ilikai.soest.hawaii.edu/uhslc/rqds.html). Geographical details (latitude, longitude) and length of data records of the tide gauge stations are listed in Table 1. This study utilizes only the historical data recorded by a tide gauge; the technical aspects of quality-control procedures of the UHSLC data have been documented in http://ilikai.soest.hawaii.edu/uhslc/rqds.html.

Sea-level variability

Climatology of annual cycle

To quantitatively evaluate the importance of the annual cycle from these data, harmonic analysis has been performed on the monthly mean sea-level time-series (Fig. 3). Harmonic analysis consists of representing the fluctuations or variations in a time series as having arisen from the adding together of a series of *sine* and *cosine* functions (Wilks 1995); harmonic analysis has commonly been used to determine the annual fluctuations of geophysical time series (see Chowdhury et al. 2007a).

The first harmonic, which represents the annual cycle, explains a considerable percentage of variance of the sea-level variability. The observed value of sea-level seasonal indices (Fig. 3 — solid lines with *shaded circle*) of most of the Hawaiian Islands, by and large displayed a strong annual cycle (Fig. 3, i-v). In most cases the first harmonic explained more than 90% of the variance. For Kahului, a combination of first and second harmonic modes explains 99% of the total variance. For two U.S-Trust Islands (Wake and Johnston), a strong annual cycle is also visible (Fig. 3, vi, vii). In all these cases, a gradual rise of sea level from May to October has been observed. Soon after the peak in September–October, a gradual recession starts.

Extremes of sea level and return calculations

Sea-level extremes for seasonal (JFM, AMJ, JAS and OND) scale on 1–100-year return periods have been plotted, with both upper and lower bounds being at 90% confidence level. These two boundaries are calculated by the bootstrap resampling method with 5,000 iterations. For simplicity, only the plots for high sea-level in Honolulu are presented (Fig. 4). The upper and lower bounds of sea-level extremes for all other stations are presented in Table 2. A

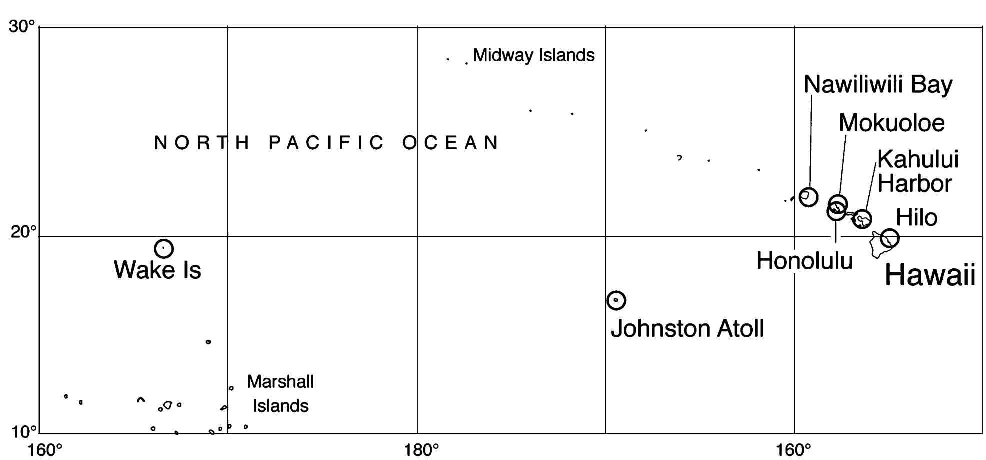

Fig. 2 Geographical locations of Hawaiian and U.S.-Trust Islands

Table 1 Geographical locations and length of data records of each tide gauge station

Islands/ Country	Tide gauge	Latitude	Longitude	Years of data records
Oahu	Honolulu	21–18N	157–52W	1905–2004
Maui	Kahului	20–54N	156–28W	1950–2004
Oahu	Mokuoloe	21–26N	157–48W	1957–2004
Kauai	Nawiliwili	21–58N	159–21W	1954–2003
Big Island	Hilo	19–44N	155–04W	1927–2004
U.S.-Trust	Wake	19–17N	166–37E	1950–2004
U.S.-Trust	Johnston	16–44N	169–32W	1947–2003

This table is reproduced from Chowdhury et al. (2008) with permission from the ASCE.

brief outline of GEV distribution and return calculations is summarized in Appendix A.

Synopsis of sea level extremes

The deviations of sea-level extremes, which are derived by subtracting the average values from the estimated sea level extremes, are presented in Table 3. Positive deviations indicate a rise from the climatological mean value, while negative deviations indicate a fall. Findings revealed that all the Hawaiian and U.S.-Trust stations are likely to experience positive deviations (extremes) in all the successive seasons on 20–100-year return periods. The deviations for

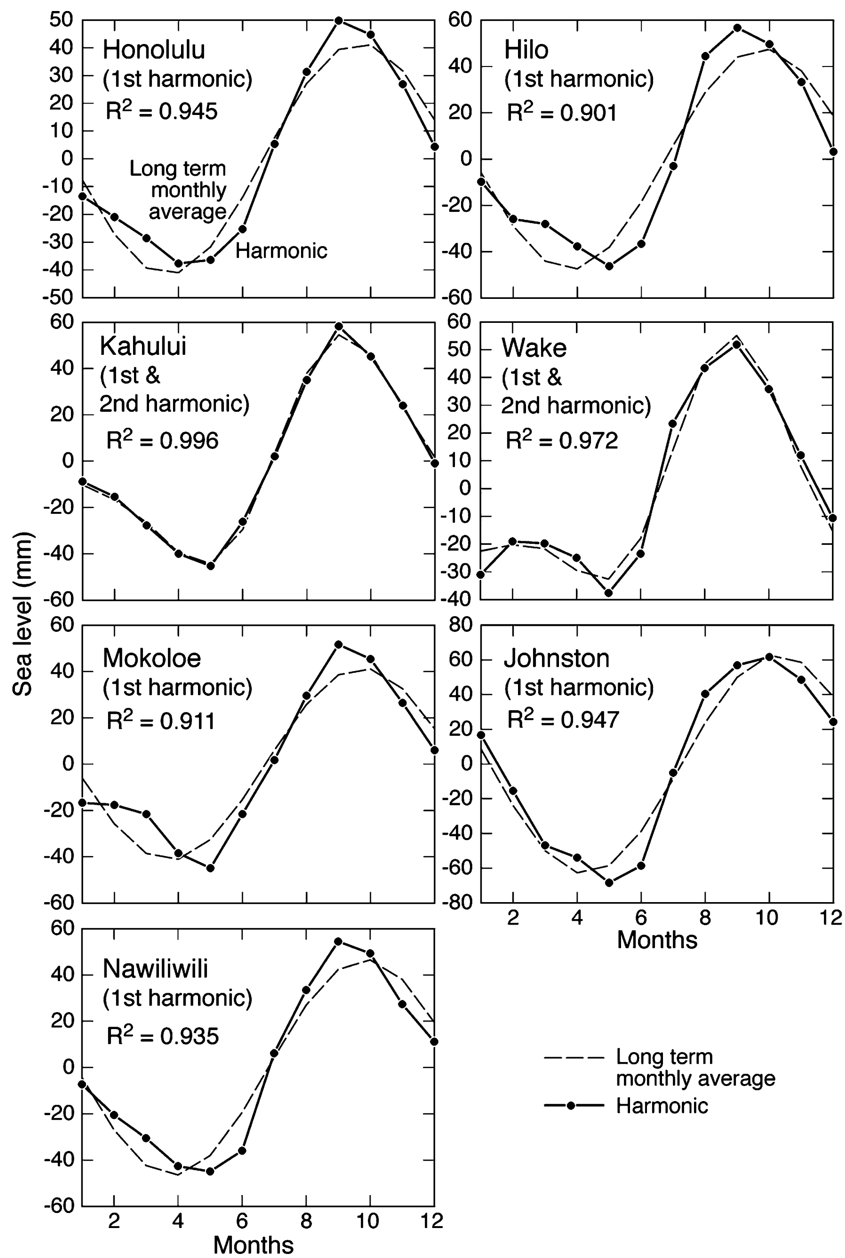

Fig. 3 1st and 2nd harmonic of sea-level variability. R^2-values are percentage of variances explained by the 1st or combination of 1st and 2nd harmonics

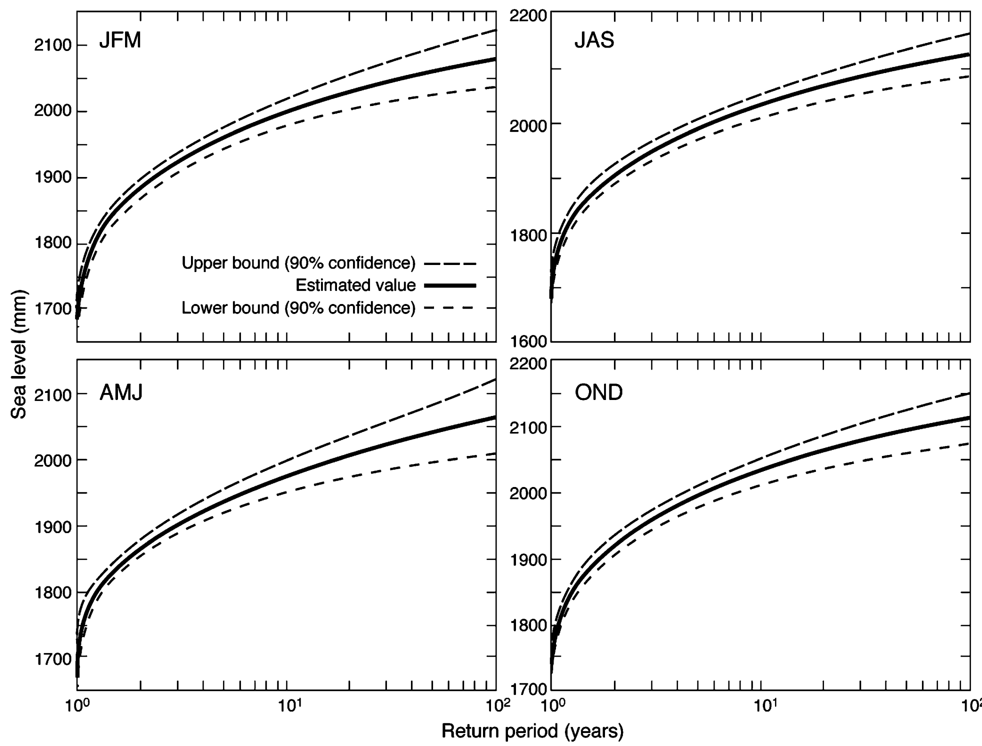

Fig. 4 The highest (maximum) sea level values at station Honolulu on seasonal (JFM, AMJ, JAS, OND) scale (at 1- to 100-years return period). The solid line shows the estimated value by analyzing the true observations. The dashed and dotted lines are the upper and lower bounds at 90% confidence level

most of the Hawaiian Islands (except Nawiliwili and Hilo) are found to be moderately elevated (100–200 mm). For the same time span, the deviations in the U.S.-Trust islands are found to be highly elevated (more than 300 mm in several seasons). Observations, from a historical perspective, revealed that any rise of 100–200 mm may cause slight local inundations; a rise greater than 300 mm can cause tidal inundations followed by increased erosion and damage to roads, harbors, and unstable sandy beaches.

On a 100-year return period, extremes of 329 mm and 547 mm are visible in the JAS season for Nawiliwili and Wake (Table 3). The reason for these high values is that some of these stations have recorded large and significant increases in their tidal range as a result of storms. Both Nawiliwili and Wake were hit by Hurricane *Iniki* in 1992. Formed during the strong El Niño of 1991–1994, *Iniki* was one of eleven Central Pacific tropical cyclones during the 1992 season. The eye of Hurricane *Iniki* passed directly over the island of Kaua'i on September 11, 1992, as a Category 4 hurricane on the Saffir-Simpson Hurricane Scale. As a result, these two stations recorded large sea-level increase in JAS. Despite increases at these two stations, other neighboring stations recorded no considerable variations caused by the same storm event. The probable reason for an abrupt rise at a specific station is that typhoons are mesoscale systems and only affect a narrow swath under the storm path. Similar observations hold for Johnston Island for the JFM season. It is therefore

Table 2 Lower and upper bounds of the sea level extremes (in mm) at 20- and 100-year return periods

Stations	Sea level extremes (mm) (100 mm=3.94 in.)							
	20-year return period				100-year return period			
	JFM	AMJ	JAS	OND	JFM	AMJ	JAS	OND
Honolulu	76~126	65~126	60~109	53~103	111~198	98~211	107~186	89~172
Kahului	99~165	93~158	77~110	96~167	106~220	120~233	89~144	133~262
Mokuoloe	89~120	84~172	75~126	87~146	90~135	128~284	92~174	113~203
Nawiliwili	90~142	85~122	80~332	73~107	109~209	116~184	98~770	94~143
Hilo	142~265	121~199	134~183	116~157	181~440	157~287	158~242	140~202
Wake	71~204	98~153	150~387	96~299	96~409	127~214	245~857	128~634
Johnston	185~356	108~166	90~189	107~165	278~649	144~243	123~337	146~248

This table is reproduced from Chowdhury et al. (2008) with permission from the ASCE

Table 3 Deviations of sea-level extremes (in mm) at 20- and 100-year return periods

Stations	Sea level deviations (mm)* (100 mm=3.94 in.)							
	20-year return period				100-year return period			
	JFM	AMJ	JAS	OND	JFM	AMJ	JAS	OND
Honolulu	102	96	86	80	152	152	145	130
Kahului	131	130	94	136	148	181	114	198
Mokuoloe	102	134	103	121	103	219	133	159
Nawiliwili	118	108	194	95	153	150	*329*	121
Hilo	201	162	161	139	288	221	196	172
Wake	132	128	270	183	221	170	*547*	*313*
Johnston	274	142	139	139	*465*	200	217	196

*Note that positive deviations indicate rise from the climatologically mean value; JFM, AMJ, JAS, and OND stands for January-February-March, April-May-June, July-August-September, and October-November-December. (This Table is reproduced from Chowdhury et al. (2008) with permission from the ASCE)

evident from the discussion that the GEV shape parameter can significantly change, making a big difference in the 20- and 100-year levels when the record contains only a few tropical cyclone events. On the basis of this observation, a fair conclusion could be drawn here: the GEV methodology has some limitations in capturing the extremes of sea level when the record contains only a few tropical cyclone events. The discussion related to GEV analysis with typhoon-affected data is still a researchable topic; here we simply present the deviations of extremes that were generated from the available time-series with typhoon-effect data for some sites.

Sea-level predictability

ENSO and sea level

ENSO usually starts to develop in summer, reaches its peak phase in the winter, and gradually weakens through the spring. Based on (i) 5-month running average of the Niño 3.4 SST and (ii) average SOI for 6-month, various studies have identified 1951, 1957–1958, 1972–1973, 1982–1983, and 1997–1998, as the strong El Niño events and 1964, 1973–1974, 1975–1976, 1988–1989, and 1998–1999 as the strong La Niña events (see http://iri.columbia.edu/climate/ENSO/background; also see Chowdhury et al. 2007a and references therein). For simplicity, we have shown here deviations of sea level for two historically strongest El Niño (1982–1983, 1997–1998) and two La Niña (1988–1989, 1998–1999) events (Fig. 5). Other strong years and other stations displayed similar trends.

The monthly average sea level of all these stations shows a trend of negative deviations during the strong El Niño events (Fig. 5). This is visible from October to June. Significantly lower-than-average sea-level was recorded in these months during the strong El Niño years. Similar, but opposite, relationships exist in La Niña years. It may be mentioned here that, unlike many other U.S.-Affiliated Pacific Islands (USAPI) (see Chowdhury et al. 2007a), the sea level of Hawaiian and U.S-Trust islands did not show strong correlations to ENSO; only some moderate correlations were visible.

To further verify the associations between the ENSO and sea level variability, lowest and highest sea level years/seasons are identified from the same time series (Table 4). The magnitudes of deviations (either positive or negative) are also marked, and then the ENSO years are superimposed. Observations revealed that the sea-level variability in Wake shows some strong correlations to ENSO, with negative deviations (fall) in all El Niño years and positive deviations (rise) in all La Niña years. In contrast, the sea-level variability in Honolulu and Hilo displays very weak correlations to ENSO.

Linear correlation of SSTs and sea level

The 3-month average sea levels for the target seasons (AMJ, JAS, OND, and JFM) for Hawiian and U.S.-Trust islands were correlated with the 3-month moving average of SSTs starting from the preceding season (JFM, AMJ, JAS, and OND). Results for two stations—Honolulu and Hilo in Hawaii (Fig. 6) and Johnston and Wake in the U.S.-Trust Island (Fig. 7)—are shown here. The positive correlation in these figures implies that warmer sea waters or more heat content with a deeper thermocline in the tropical North-Central Pacific correspond to higher sea level in these areas. Conversely, negative sea-level anomalies are associated with cooler sea waters or less heat content in the North-Central Pacific.

In Honolulu, the sea level (SL) in JAS and OND displays good correlation with the SSTs of the preceding

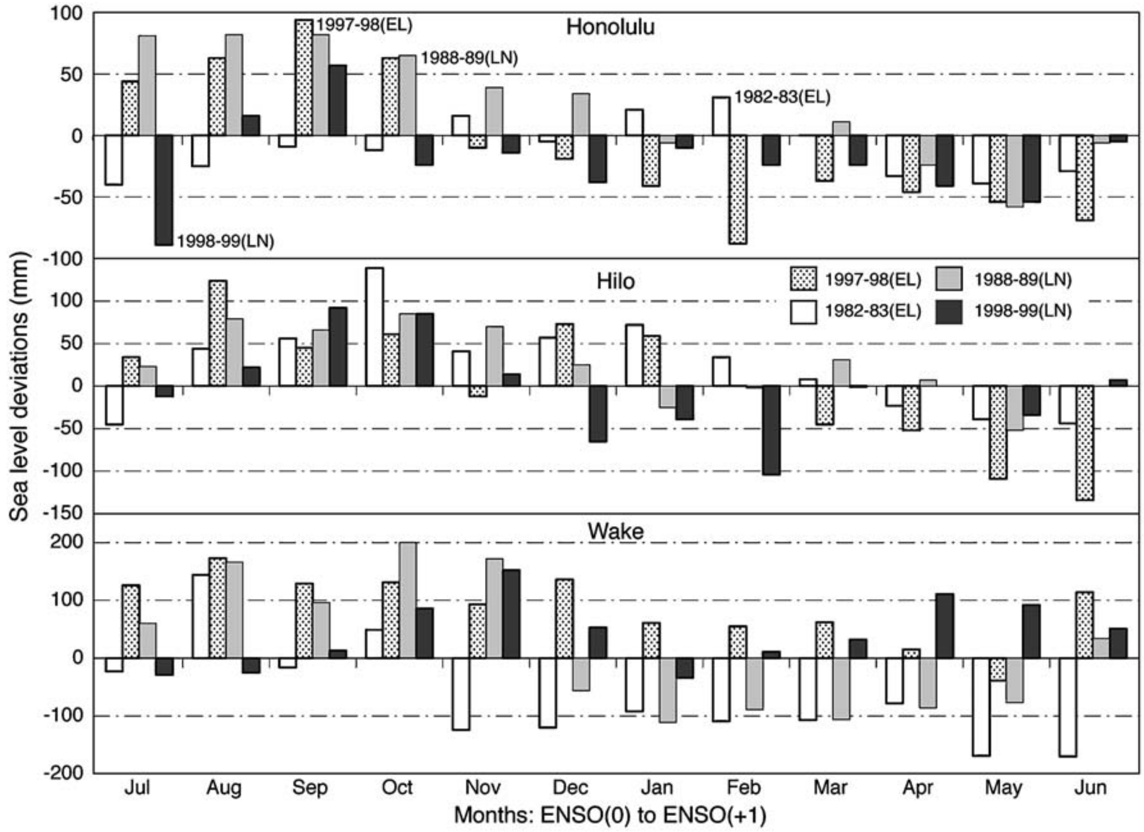

Fig. 5 Composites of monthly sea-level deviations for Honolulu, Hilo, and Wake during major El Niño (EL) and La Niña (LN) years

seasons AMJ and JAS [Fig. 6 (ii), (iii)]. A region of positive correlation (horseshoe shape) is distinct in the tropical western Pacific extending up to 140E, and a region of negative correlation exists in the Niño 3.4 area. Some marginal positive association (also of horseshoe shape) has also been observed between OND sea-level and SSTs of the following year (+JFM) [Fig. 6 (iv)]. As observed in the correlation maps [Fig. 6 (iii, iv)], part of the tropical

Table 4 Lowest and highest sea-level years/seasons

Stations	Lowest sea level				Highest sea level			
	Year	Season	Deviations (mm)	Remarks (EN/LN)	Year	Season	Deviations (mm)	Remarks (EN/LN)
Honolulu	1990	JFM	−112.5	EN	2003	JAS	+133.0	EN
	1997	JFM	−102.5	EN[b]	1981	JAS	+123.0	n/a
	1986	AMJ	−100.0	EN	1984	OND	+119.7	LN
	1976	JFM	−81.3	EN[b]	1995	OND	+107.0	LN
	1982	AMJ	−70.7	EN[b]	2004	OND	+102.0	EN
Hilo	1975	AMJ	−128.0	EN	2004	JAS	+133.3	EN
	1977	AMJ	−126.7	EN	1996	JAS	+112.7	LN
	1976	JFM	−125.3	EN	2003	JAS	+109.3	EN
	2000	JFM	−99.7	LN	1984	JAS	+94.3	LN
	1998	AMJ	−98.3	LN	2005	JFM	+91.0	EN
Wake	1992	AMJ	−152.7	EN[a]	1996	JAS	+174.3	LN
	1983	AMJ	−139.0	EN	2000	JAS	+147.0	LN
	1977	JFM	−129.0	EN	1995	JAS	+146.0	LN
	1989	JFM	−102.0	LN	1981	JAS	+144.5	n/a
	1979	AMJ	−99.7	n/a	1997	JAS	+142.7	LN

[a] Note that EN and LN stands for El Niño and La Niña years, and JFM, AMJ, JAS, and OND stands for January-February-March, April-May-June, July-August-September, and October-November-December.
[b] Strong event

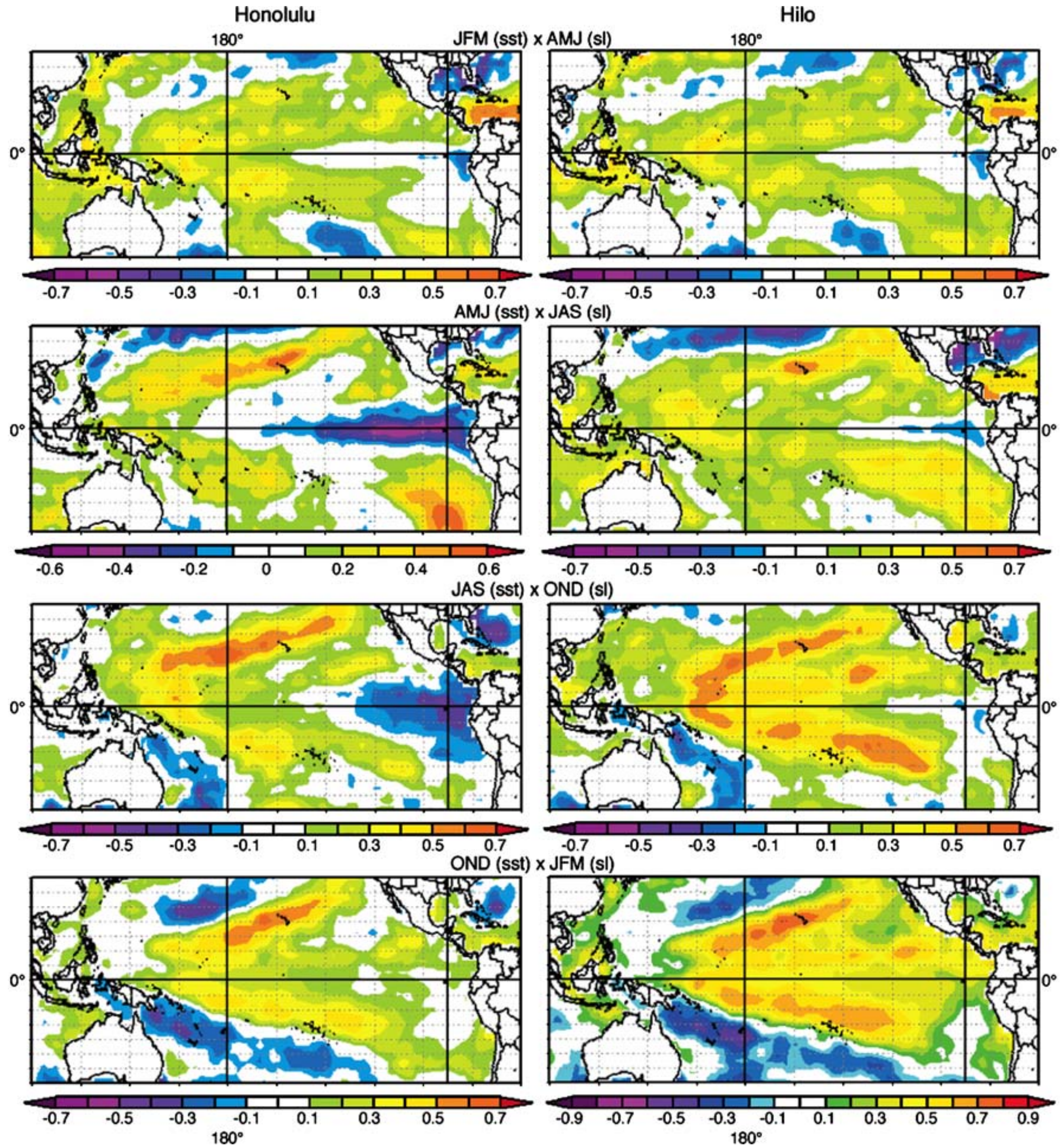

Fig. 6 Linear correlation between seasonal SST across the tropical Pacific and sea levels (SL) in the Hawaiian Islands [Honolulu *(left panel)* and Hilo *(right panel)*]

western Pacific SSTs (140W-160E; 15N — 25N) also displayed strong positive correlation (0.5–0.7) to sea level at these two stations. In the case of Hilo, the correlation maps for OND (SL) and JFM (SL) display some important positive correlations (0.4–0.9) in the region of 120W-140E [Fig. 6 (vii) and (viii)]. In both of these cases, the local SSTs appear to be in phase with sea-level variations.

Other stations at Kahului, Mokuoloe, and Nawiliwili also display similar correlations; the correlation maps for Mokuoloe and Nawiliwili correspond well to those of Honolulu while Kahului corresponds better with Hilo. Observation also revealed that the AMJ (SST) and JAS (SL) maps for Nawiliwili and Kahului display (not shown) a region, bounded by 110E-110W and 20N-40N, of very high negative correlation (0.5–0.7).

Considering the other stations at Johnston and Wake, the OND (SL) and JFM (SL) of Johnston display some weak to moderate positive correlations with JAS (SST) and OND (SST) [Fig. 7 (iii–iv)]. There are no specific regions of distinct positive or negative correlations. However, Wake provided some interesting correlation maps for SSTs in JFM and JAS and for sea levels in AMJ and OND respectively. The variability of AMJ (SL) shows very strong negative correlation (0.5–0.7) with the preceding

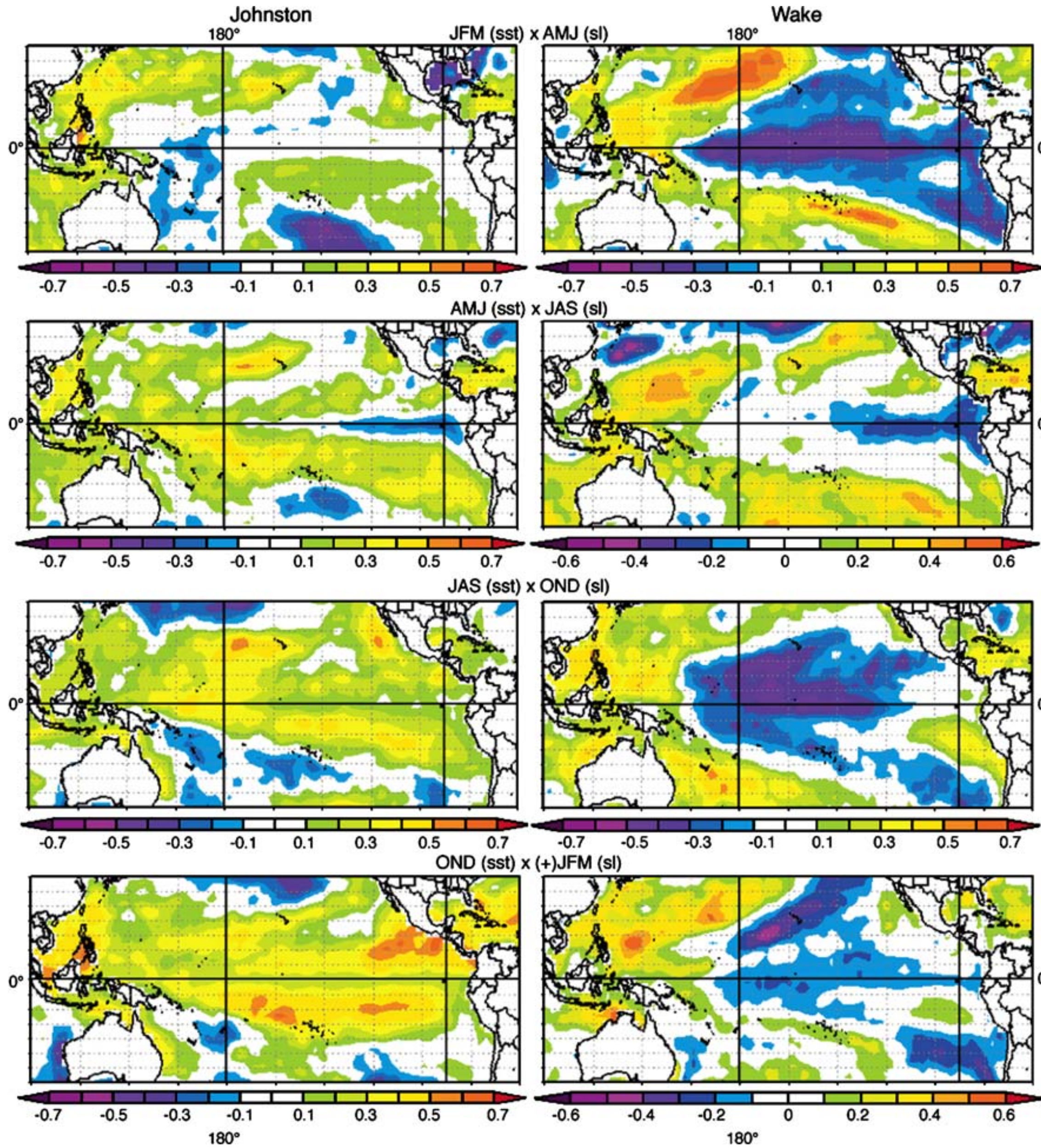

Fig. 7 Same as Fig. 6, except for U.S.-Trust Islands [Johnston *(left panel)* and Wake *(right panel)*]

JFM (SST) in the Niño 3.4 area [Fig. 7 (v)]. A region of positive correlation is also visible between 160E-160W and 15N-30N. While the AMJ (SST) and JAS (SL) map shows no interesting features, the JAS (SST) and OND (SL) again show an active Niño 3.4 area with negative association [Fig. 7 (vii)]. The local SSTs seem to be in phase with sea-level variations here.

It has been interestingly observed that, among the correlation maps, only Wake shows some features that resemble ENSO [Fig. 7 (v), (vii)]. It is important to mention here that Wake is the only island in this study from the west of the dateline (DL). Therefore, it seems that the sea-level variability of the islands located west of the DL (i.e., Wake) is more sensitive to ENSO than the locations to the east of the DL (i.e., Honolulu, Hilo, Johnston, and others). Also it is notable that only Wake shows some strong correlations to ENSO, with negative deviations (fall) in all El Niño years and positive deviations (rise) in all La Niña years). Previous studies of Chowdhury et al. (2007a, b) also support this finding by showing that sea level variability in the U.S-Affiliated Pacific Island (USAPI) communities that are located west of the DL and across the northwestern Pacific Ocean, is very sensitive to ENSO cycle with low sea-level in El Niño and high sea-level in La Niña years.

CCA model forecast and hindcast skill for seasonal maxima

As one of the goals of this study is to help forecast sea level maxima on seasonal time-scales, exploiting PEAC's experience with a similar forecasting scheme in other regions (see Chowdhury et al. 2007b), a canonical correlation analysis (CCA) statistical model has been developed. The hindcast skill of the CCA model for 1950–2004 is estimated using a cross-validated scheme. The CCA cross-validation skill is a measure of forecast quality. If the skill lies between 0.3 and 0.4 then the forecasts are thought to be somewhat useful. Higher skills correspond to greater expected accuracy of the forecasts. Forecasts are thought to be 'fair' if the skill level is closer or greater than 0.4, it is said to be 'good' when the skill level is greater than 0.5, and the skill is treated as 'very good' when the skill level is closer or greater than 0.7. This CCA method has been described extensively in the literature (see Barnston and He 1996; Chu and He 1994; Cherry 1996; Newman and Sardeshmukh 1995 and references therein) and is not discussed further here. A short summary of some of the most interesting findings follows.

To provide a predictive skill at longer lead time, CCA cross-validation skills up to three seasons in advance are calculated; the average skills at 0–3 seasons lead time for different islands (Fig. 8) show different levels of predictive skill. In general the forecast skills for Honolulu, Kahului, and Hilo are fairly good with average CCA correlation skills of 0.333, 0.401, and 0.499 at 1–3 seasons lead time, respectively. The skill is considerably better at 0-season lead time. Among all the islands, the average predictive skill for Hilo has been found to be strongest (0.506, 0.520, 0.486, and 0.486) at 0 to 3-seasons lead time. Predictive skill for other stations in the Hawaiian Islands (Nawiliwili and Mokuoloe) displayed poor skill (<0.30). Of the two other U.S.-Trust islands, Wake displayed relatively better skill (0.2–0.4), but Johnston Island provided very poor skill.

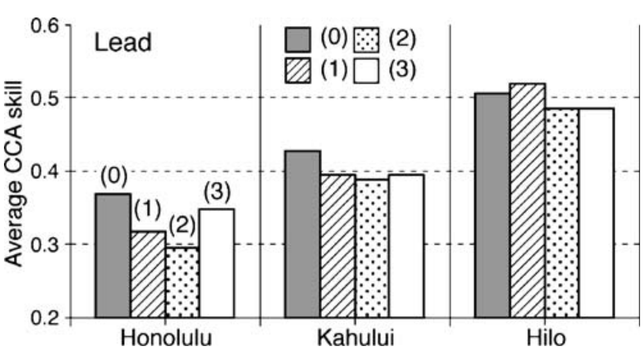

Fig. 8 Average CCA cross-validation hindcast skills at 0–3 seasons lead time. Note that Lead 0, 1, 2, and 3 indicates 'sea-level' of target season (say for example, JFM) based on SSTs of previous seasons OND (lead 0), JAS (lead 1), AMJ (lead 2), and JFM (lead 3) respectively

Global sea-level rise and potential implications in Hawaiian islands

The recent IPCC report on climate change illustrates that global average sea level rose at an average rate of 1.8 [1.3–2.3] mm per year from 1961 to 2003 (IPCC 2007a). The rate was faster from 1993 to 2003: about 3.1 [2.4 to 3.8] mm per year (also see, for example, Rhamstorf (2007); Otto-Bliesner et al. (2006); and Overpeck et al. (2006)]. The IPCC report has already projected that coasts will be exposed to increasing risks, including coastal erosion, due to climate change and sea-level rise (IPCC 2007b). The effect will be exacerbated by increasing human-induced pressures on coastal areas. By the 2080's, many millions more people are projected to be flooded every year due to sea-level rise. Those densely populated and low-lying areas where adaptive capacity is relatively low, and which already face other challenges such as tropical storms or local coastal subsidence, are especially at risk. The numbers affected will be largest in the mega-deltas of Asia and Africa, and small islands (Hawaii and others) are equally vulnerable.

Findings of this study have clearly demonstrated that projected extremes in global sea-level rise are expected to have a number of profound impacts on coastal systems in the Hawaiian and other Pacific islands. Such impacts include increased coastal and beach erosion, higher and more frequent storm-surge flooding with more extensive coastal inundation, changes in surface-water quality and groundwater availability, increased loss of property and coastal habitats, increased flood risk and potential loss of life, loss of cultural resources and values, impacts on agriculture and aquaculture through decline in soil and water quality, and loss of tourism, recreation, and transportation functions. Many of these impacts will be severely detrimental to many major coastal island communities and ecosystems.

At present it is difficult to build a definitive relationship between sea level rise and erosion at specific locations because of the considerable variability in slope, beach width and geomorphology along the coast. While the *Bruun Rule* (Bruun 1962) is commonly used in many places (Samantha and Kenneth 2007) to develop a generic ratio for sea-level rise to shoreline retreat, the conditions in Hawaii don't particularly satisfy the prerequisites for applying the Bruun Rule. However, there are studies that can provide a guideline for predictive accuracy of shoreline change rate methods for Hawiian Islands (Genz et al. 2007; Dolan et al. 1991). Despite these efforts, coastal damage scenarios based on extremes of sea-level and shoreline change for the Hawaiian Islands are still a challenging task. The unpredictability of periodic storm effects, land subsidence, coastal stabilization, and the influence of inlets further complicate the problem. More research is needed here to develop a comprehensive picture of damage threat, possible impact, and vulnerable infrastructures.

Summary and conclusions

Coastal hazards management will need the integration of weather and climate monitoring into the process. Therefore, expanding our capability in areas of observing the ocean and the atmosphere for accurate and timely forecasts of extreme sea level is necessary.

One of the important findings from this study is that typhoon-affected data (Nawiliwili, Wake, and Johnston) can significantly change the GEV shape parameters, making a big difference in the year level. If other stations had a similar direct hit in the past 100 years their GEV curves may resemble the same curves as Nawiliwili, Wake, and Johnston. Therefore, a fair conclusion could be drawn that GEV methodology has some limitations in capturing the extremes of sea level when the record contains only a few tropical cyclone events. However, despite this limitation, the GEV model has been found to be instrumental in generating advance information for sea level extremes on seasonal and long-term time scales. This is an important knowledge base for coastal hazards management decision analyses in the Hawaiian and U.S.-Trust islands. At the same time, it is also true that other stations might experience the same storm surges in the future. Therefore, the extreme events of Nawiliwili, Wake, and Johnston should be seen as a problem for the whole region, and a unified regional planning approach for coastal hazard management is essential to tackle this problem.

While ENSO is the largest source of year-to-year climate variability, our observations have revealed that, because of weak teleconnections, a skillful ENSO-based sea-level forecast is difficult for some of the islands. However, the SST-based sea-level forecasts provided a better result, but still not as skillful as expected. Therefore, we emphasize the need for further studies with additional oceanic/atmospheric variables (indices) to raise the predictive skill.

In the future, Arctic warming and the melting of polar glaciers will be considerable. This is one of the most pressing global research problems for policy and planning analysis and is currently one of the most intensely studied fields related to global climate change. Increased vulnerability to flooding inundation and coastal hazards will necessitate a new planning initiative to managing these risks.

Acknowledgments This project was funded by cooperative agreement NA17RJ1230 between the Joint Institute for Marine and Atmospheric Research (JIMAR) and the National Oceanic and Atmospheric Administration (NOAA). The views expressed herein are those of the authors and do not necessarily reflect the views of NOAA or any of its subdivisions. We are grateful to the anonymous reviewers for their valuable comments. Thanks to Mr. Dolan Eversole for his report (personal communication) that provided many valuable policy insights. Grateful acknowledgements are due to Dr. Cheryl Anderson, and Sarah Jones. We are thankful to Diane J Henderson for proof editing and Nancy Hulbirt for editing figures. Thanks are also due to the American Society of Civil Engineers (ASCE) for giving us permission to reproduce Tables 1, 2, 3 and Figs. 2, 3, 4 from Chowdhury et al. (2008).

Appendix A

Probability distribution function (PDF) of GEV:

$$f(x) = \frac{1}{\beta}\left[1 + \frac{\kappa(x-\zeta)}{\beta}\right]^{1-1/\kappa} \exp\left\{-\left[1 + \frac{\kappa(x-\zeta)}{\beta}\right]^{-1/\kappa}\right\}, \quad 1 + \frac{\kappa(x-\zeta)}{\beta} > 0 \tag{1}$$

The cumulative distribution function (CDF) of GEV:

$$F(x) = \exp\left\{-\left[1 + \frac{\kappa(x-\zeta)}{\beta}\right]^{-1/\kappa}\right\} \tag{2}$$

And the return period R(x):

$$R(x) = \frac{1}{[1 - F(x)]} \tag{3}$$

There are three parameters in these equations: a location (or shift) parameter ζ, a scale parameter β, and a shape parameter κ. We need to estimate all these three parameters. The method of L-moments was chosen to estimate these parameters:

$$\kappa = 7.859c + 2.9554c^2, c = \frac{2}{3+\tau_3} - \frac{\log 2}{\log 3}, \tau_3 = \frac{l_3}{l_2}$$

$$\beta = \frac{l_2 \kappa}{(1 - 2^{-\kappa})\Gamma(1+\kappa)}$$

$$\zeta = l_1 - \beta[1 - \Gamma(1+\kappa)]/\kappa$$

Where l_1 is the L-location or mean of the distribution, l_2 is the L-scale, and τ_3 is the L-skewness (Hosking and Wallis 1997).

Finally, the bootstrap resampling technique was adapted to estimate the sampling uncertainty of the return values (see Gnedenko 1943; Efron and Tibshirani 1993; Chu and Wang 1997; Zwiers and Kharin 1998; Katz et al. 2002; Mendez et al. 2007; and Chu et al. 2008 for a comprehensive treatment of GEV).

References

Barnston AG, He Y (1996) Skill of CCA forecasts of 3-month mean surface climate in Hawaii and Alaska. J Clim 9:2020–2035. doi:10.1175/1520-0442(1996)009<2020:LLFOSP>2.0.CO;2

Bruun P (1962) Sea level rise as a cause of shore erosion. J Wtrwy and Harb Div 1:116–130

Bjerknes J (1966) A possible response of the atmospheric Hadley circulation to equatorial anomalies of ocean temperature. Tellus 18:820–829

Bjerkness J (1969) Atmospheric teleconnections from the equatorial Pacific. Mon Weather Rev 97:163–172. doi:10.1175/1520-0493(1969)097<0163:ATFTEP>2.3.CO;2

Cherry S (1996) Singular value decomposition analysis and canonical correlation analysis. J Clim 9:2003–2009. doi:10.1175/1520-0442(1996)009<2003:SVDAAC>2.0.CO;2

Chowdhury MR, Chu P-S, Schroeder T (2007a) ENSO and seasonal sea-level variability—A diagnostic discussion for the U.S-affiliated Pacific Islands. Theor Appl Climatol 88:213–224. doi:10.1007/s00704-006-0245-5

Chowdhury MR, Chu P-S, Schroeder T, Colasacco N (2007b) Seasonal sea level forecasts by canonical correlation analysis: an operational scheme for the U.S.-. Affiliated Pac Islands. Int J Climatol 27:1389–1402

Chowdhury MR, Chu P-S, Zhao X, Schroeder T (2008) Sea-level extremes and challenges to manage coastal hazards in the vicinity of Hawaiian Islands. In: Wallendorf L, Ewing L, Jones C, Jaffe B (eds) Solutions to coastal disasters 2008, Published by the American Society of Civil engineers, ISBN-0-7844-0978-7, page. 28–37

Chu P-S (1995) Hawaii rainfall anomalies and El Nino. J Clim 8:1697–1703. doi:10.1175/1520-0442(1995)008<1697:HRAAEN>2.0.CO;2

Chu P-S, Chen H (2005) Interannual and interdecadal rainfall variations in the Hawaiian Islands. J Clim 18:4796–4813. doi:10.1175/JCLI3578.1

Chu P-S, He Y (1994) Long-range prediction of Hawaiian winter rainfall using canonical correlation analysis. Int J Climatol 14:659–669. doi:10.1002/joc.3370140605

Chu P-S, Wang J (1997) Tropical cyclone occurrences in the vicinity of Hawaii: are the difference between El Niño and non-El Niño years significant? J Clim 10:2683–2689. doi:10.1175/1520-0442(1997)010<2683:TCOITV>2.0.CO;2

Chu P-S, Zhao X, Ruan Y, Grubbs M (2008) Extreme rainfall events in the Hawaiian Islands. J Appl Meteorol Climatol (Forthcoming)

Dolan R, Fenster MS, Holme SJ (1991) Temporal analysis of shoreline recession and accretion. J Coast Res 7(3):723–744

Efron B, Tibshirani RJ (1993) An introduction to the bootstrap. Chapman and Hall, 436 pp

Genz AS, Fletcher CH, Dunn RA, Frazer LN, Rooney JJ (2007) The predictive accuracy of shoreline change rate methods and alongshore beach variation on Maui, Hawaii. J Coast Res 23 (1):87–105. doi:10.2112/05-0521.1

Gnedenko B (1943) Sur la distribution limite du terme maximum d'une se'rie ale'atoire. Ann Math 44:423–453. doi:10.2307/1968974

Hosking JRM, Wallis JR (1997) Regional frequency analysis: an approach based on *L*-moments. Cambridge University Press, New York, 224 pp

IPCC (2007a) Climate change 2007: the physical basis—summary for policymakers. Working group I to the fourth assessment report of the Intergovernmental Panel on Climate Change (IPCC) (available at: www.ipcc.ch/SPM2avr07.pdf)

IPCC (2007b) Climate change 2007: climate change impacts, adaptation and vulnerability—summary for policymakers. Working group II to the fourth assessment report of the Intergovernmental Panel on Climate Change (available at: http://www.ipcc.ch/SPM13apr07.pdf.)

Katz RW, Parlange MB, Naveau P (2002) Statistics of extremes in hydrology. Adv Water Resour 25:1287–1304. doi:10.1016/S0309-1708(02)00056-8

Mendez FJ, Menedez M, Luceno A, Losada I (2007) Analyzing monthly extremes sea levels with a time-dependent GEV model. J Atmos Ocean Technol 24:894–911. doi:10.1175/JTECH2009.1

Newman M, Sardeshmukh PD (1995) A caveat concerning singular value decomposition. J Clim 8:352–360. doi:10.1175/1520-0442(1995)008<0352:ACCSVD>2.0.CO;2

Otto-Bliesner B et al (2006) Simulating arctic climate warmth and ice field retreat in the last interglaciation. Science 311:1751–1753

Overpeck J et al (2006) Paleoclimatic evidence for future ice-sheet instability and rapid sea-level rise. Science 311:1747–1750

Richmond BM, Fletcher CH, Grossman EE, Gibbs AE (2001) Islands at risk: coastal assessment and mapping in the Hawaiian Islands. Environ Geosciences 8(1):21–37. doi:10.1046/j.1526-0984.2001.008001021.x

Rhamstorf S (2007) A semi-empirical approach to projecting future sea level rise. Science 315:368–370. doi:10.1126/science.1135456

Ropelewski CF, Halpert MS (1987) Global and regional scale precipitation patterns associated with the El Niño—Southern oscillation. Mon Weather Rev 115:1606–1626. doi:10.1175/1520-0493(1987)115<1606:GARSPP>2.0.CO;2

Samantha ES, Kenneth P (2007) Implications of sea level rise for coastal dune habitat conservation in Wales, UK. J Coast Conserv 11:31–52

Wilks DS (1995) Statistical methods in the atmospheric sciences. Academic Press, 467 pp

Yu Z-P, Chu P-S, Schroeder T (1997) Predictive skills of seasonal to annual rainfall variations in the U. S. affiliated Pacific islands: canonical correlation analysis and multivariate principal component regression approaches. J Clim 10:2586–2599. doi:10.1175/1520-0442(1997)010<2586:PSOSTA>2.0.CO;2

Zwiers FW, Kharin VV (1998) Changes in the extremes of the climate simulated by CCC GCM2 under CO2 Doubling. J Clim 11:2200–2222. doi:10.1175/1520-0442(1998)011<2200:CITEOT>2.0.CO;2